

## Mass and Energy Distributions in the Spontaneous Fission of Some Heavy Isotopes\*

REINHARD BRANDT,† STANLEY G. THOMPSON, RAYMOND C. GATTI, AND LLAD PHILLIPS‡

*Lawrence Radiation Laboratory, University of California, Berkeley, California*

(Received 1 April 1963)

A back-to-back semiconductor counter system was used to study the energy and mass distributions of the fission fragments in the spontaneous fission of the isotopes,  $\text{Fm}^{254}$ ,  $\text{E}^{253}$ ,  $\text{Cf}^{254}$ , and  $\text{Cm}^{248}$ . The results are compared to the fission fragments produced by the spontaneous fission of  $\text{Cf}^{252}$ , whose fission properties are well known. All distributions (including those of the odd-mass isotope  $\text{E}^{253}$ ) are rather similar, but not identical with the standard  $\text{Cf}^{252}$ . The mean prompt kinetic energy of the fragments increases with  $Z$ , and this trend is compared with the results of other related experiments. The asymmetry of the mass distributions shows only small differences between the isotopes studied here. Some theoretical aspects of the asymmetries are discussed. The variance (widths) of nearly all the distributions increases with  $Z$  and seems to increase with  $A$ . A new semiempirical correlation between the variances and  $Z^2/A$  is proposed and interpreted on a qualitative basis. The effects of neutron emission on the results are briefly discussed and the values of the mean total kinetic energy release are corrected for the effect of neutron emission.

### I. INTRODUCTION

IN this work we describe measurements of the spontaneous-fission properties of several heavy isotopes. Data are compiled and discussed in such a way as to reveal the most significant features of the results. The value of such a study is to provide experimental data from which some general features of the fission process may be deduced and against which theories may be tested, both generally and in detail.

Prior to this work, very little information has been available concerning details of spontaneous-fission isotopes other than  $\text{Cf}^{252}$ .<sup>1</sup> Therefore, such properties as the mass-yield curves, kinetic-energy distributions, and their widths remained to be studied for a number of heavy nuclei.

Such investigations have become possible during the past few years because of advancements in several directions. The first involved production of larger amounts of certain heavy isotopes by multiple neutron capture in high-flux reactors. The second involved application of semiconductor counters for energy measurements. The third development was the availability of multidimensional pulse-height analyzers which allow one to record and store information correlating, for example, two energy measurements from each event. The fourth advancement is the ready availability of computers for calculating the results of a very large number of measurements.

In the experiments reported here, the energies of both fragments from spontaneous-fission events were studied for several isotopes. From these energies the masses of the fission fragments and total kinetic energies were calculated. The properties of the measured dis-

tributions were compared with those of the isotope  $\text{Cf}^{252}$ , measured under the same conditions. Trends in the properties as functions of  $Z$  and  $A$  and certain fission parameters were studied.

### II. EXPERIMENTAL PROCEDURES

Transcurium isotopes used in these experiments were produced by long-time irradiation of curium isotopes with neutrons. As a result, elements as heavy as fermium were produced.<sup>2</sup> The production paths are shown schematically in Table I. The elements were separated on ion-exchange columns.<sup>3</sup> Special care was taken to remove all contaminations to such a level that their influence could be neglected in the final results. The isolated and purified isotopes were electro-deposited on approximately 5- $\mu$ m-thick Ni foils. The measured foil thicknesses are given in Table I.

The foils were placed between two back-to-back phosphorus-diffused guard-ring-type silicon semiconductor counters<sup>4</sup> by means of which the energies of both fragments from fission events were measured. The energies of both fission fragments were recorded by utilizing standard electronic equipment. The binary equivalent values of those energies were stored on paper tape. Data recorded on paper tape were then transferred to magnetic tape in a form that retained the identity of each fission event and was directly acceptable by the IBM-7090 computer.

The fission fragments from the spontaneous fission of  $\text{Cf}^{252}$  were used for energy calibration of the semiconductor detectors. Kinetic energies of the fission fragments from spontaneous fission of  $\text{Cf}^{252}$  have been determined independently by time-of-flight measure-

\* This work was done under the auspices of the U. S. Atomic Energy Commission.

† Present address: CERN, Geneva 23, Switzerland.

‡ Present address: 83-1/2 Appleton, Arlington, Massachusetts.

<sup>1</sup> E. K. Hyde, Lawrence Radiation Laboratory Report UCRL-9036 revised, 1962 (unpublished).

<sup>2</sup> S. Fried and H. Schumacher, Lawrence Radiation Laboratory Report UCRL-10023, 1962 (unpublished).

<sup>3</sup> R. Brandt, Ph.D. thesis, Lawrence Radiation Laboratory Report UCRL-10481, 1962 (unpublished).

<sup>4</sup> F. S. Goulding and W. L. Hansen, Nucl. Instr. Methods 12, 249 (1961).

TABLE I. Some experimental details concerning the investigated isotopes.

Isotope	Fm <sup>254</sup>	E <sup>253</sup>	Cf <sup>254</sup>	Cf <sup>250</sup>	Cm <sup>248</sup>
Production path	E <sup>253</sup> ( <i>n</i> , $\gamma$ ) Fm <sup>254</sup> ( <i>m</i> ) $\xrightarrow{\beta^-}$	Cf <sup>253</sup> $\xrightarrow{\beta^-}$ E <sup>253</sup>	E <sup>253</sup> ( <i>n</i> , $\gamma$ ) E <sup>254</sup> ( <i>m</i> ) $\xrightarrow{\text{e.c.}}$ Cf <sup>254</sup>	E <sup>254</sup> $\xrightarrow{\alpha}$ Bk <sup>250</sup> $\xrightarrow{\beta^-}$ Cf <sup>250</sup>	Cf <sup>252</sup> $\xrightarrow{\alpha}$ Cm <sup>248</sup>
Approximate activity at start of experiment (fissions/min)	4000	4	40	5	400
Total events recorded	81 900	11 800	83 800	12 100	70 000
Fraction of events due to other fission activities (fission %)	<0.1	$\leq 6$ Cf <sup>252</sup> $\leq 6$ E <sup>254</sup>	4 Cf <sup>250</sup> 2 Cf <sup>252</sup>	1.5 E <sup>254</sup> $\leq 4$ Cf <sup>252</sup>	(5 $\pm$ 1) Cm <sup>244</sup>
Half-life	3.2 h	20.0 day	60.5 day <sup>a</sup>	13 yr <sup>a</sup>	4.7 $\times$ 10 <sup>5</sup> yr
Ni-foil thickness (in $\mu\text{g}/\text{cm}^2$ )					
source	140 $\pm$ 10	240	170 $\pm$ 10	210	210
Cf <sup>252</sup> standard	170	210	150	220	210

<sup>a</sup> L. Phillips, R. C. Gatti, R. Brandt, and S. G. Thompson, Lawrence Radiation Laboratory Report UCRL-10464, 1962 (unpublished).

ments.<sup>5</sup> Therefore, absolute values for the most probable light and heavy fission-fragment energies are known. (Further details are discussed in Appendix A.) It was assumed that the "pulse-height defect" as described recently by several authors<sup>6</sup> was the same for all the isotopes investigated.

The stability of the apparatus was checked as follows. First, the positions of the most probable light and heavy fission fragments of the Cf<sup>252</sup> standard were determined before and after each experiment. In addition, the stability of the electronic equipment during the experiment was checked continuously with pulses from a mercury pulser. Corrections were made for instabilities in the electronic system.

The Fm<sup>254</sup> experiment was completed during the relatively short time of 2 days. The Cf<sup>254</sup> experiment lasted several weeks, and several different sets of semiconductor detectors which all gave similar results were used. The Cf<sup>250</sup> experiments were carried out with a rather small source of 5 fission/min, as compared to 4000 fissions/min used at the start of the Fm<sup>254</sup> experiment. The solid-state detectors used for this experiment were relatively poor. This accounts for the large uncertainties in the results for this isotope as shown in a following section. The Cm<sup>248</sup> experiment was carried out with two different electronic techniques, both giving essentially the same results. The first was similar to those used for Fm<sup>254</sup>, Cf<sup>254</sup>, and Cf<sup>250</sup>; the second

TABLE II. Properties of the energy and mass distributions.

	Fm <sup>254</sup>	E <sup>253</sup>	Cf <sup>254</sup>	Cf <sup>252</sup>	Cf <sup>250</sup>	Cm <sup>248</sup>
$\langle E_H \rangle^a$	81.7 $\pm$ 1.0	81.6 $\pm$ 1.5	79.5 $\pm$ 1.0	78.2 $\pm$ 0.2	79.0 $\pm$ 1.5	76.5 $\pm$ 1.0
$\langle E_L \rangle^b$	104.0 $\pm$ 1.0	103.4 $\pm$ 1.5	102.1 $\pm$ 1.0	102.2 $\pm$ 0.2	103.5 $\pm$ 1.5	100.0 $\pm$ 0.8
$\langle E_T \rangle^c$	186 $\pm$ 2	185 $\pm$ 3	182 $\pm$ 2.0	180.4 $\pm$ 0.5	182.5 $\pm$ 3	176.5 $\pm$ 2.0
$\langle E_K \rangle^d$	189 $\pm$ 2	188 $\pm$ 3	185 $\pm$ 2	183.0 $\pm$ 0.5	185 $\pm$ 3	179 $\pm$ 2
$\langle M_L \rangle^e$	111.5 $\pm$ 0.3	111.3 $\pm$ 0.5	110.9 $\pm$ 0.4	109.1 $\pm$ 0.2	108.0 $\pm$ 0.4	107.3 $\pm$ 0.3
$\langle M_H \rangle^f$	142.5 $\pm$ 0.3	141.7 $\pm$ 0.5	143.0 $\pm$ 0.4	142.9 $\pm$ 0.2	141.9 $\pm$ 0.4	140.7 $\pm$ 0.3
$\sigma^2(E_H)-d^g$	85 $\pm$ 2 (64 $\pm$ 2)	94 $\pm$ 5 (71 $\pm$ 4)	71 $\pm$ 3 (61 $\pm$ 2)		81 $\pm$ 5 (81 $\pm$ 5)	64 $\pm$ 3 (68 $\pm$ 3)
$\sigma^2(E_H)-n^h$	85 $\pm$ 3	87 $\pm$ 7	74 $\pm$ 4	64	64 $\pm$ 7	60 $\pm$ 5
$\sigma^2(E_L)-d$	43 $\pm$ 2 (39 $\pm$ 2)	49 $\pm$ 3 (45 $\pm$ 2)	46 $\pm$ 2 (45 $\pm$ 2)		55 $\pm$ 4 (55 $\pm$ 4)	42 $\pm$ 2 (43 $\pm$ 2)
$\sigma^2(E_L)-n$	43 $\pm$ 3	43 $\pm$ 4	40 $\pm$ 3	39	39 $\pm$ 6	38 $\pm$ 3
$\sigma^2(E_T)-d$	138 $\pm$ 4 (110 $\pm$ 3)	165 $\pm$ 8 (130 $\pm$ 4)	126 $\pm$ 6 (112 $\pm$ 4)		146 $\pm$ 8 (146 $\pm$ 5)	132 $\pm$ 4 (133 $\pm$ 3)
$\sigma^2(E_T)-n$	138 $\pm$ 5	145 $\pm$ 10	124 $\pm$ 8	110	110 $\pm$ 10	109 $\pm$ 5
$\sigma^2(M)-d$	61 $\pm$ 2	66 $\pm$ 4	58 $\pm$ 3		64 $\pm$ 4	58 $\pm$ 2
(one branch)	(52 $\pm$ 2)	(57 $\pm$ 2)	(53 $\pm$ 2)		(66 $\pm$ 2)	(60 $\pm$ 2)
$\sigma^2(M)-n$	52 $\pm$ 3	52 $\pm$ 5	48 $\pm$ 4	43	41 $\pm$ 5	41 $\pm$ 3

<sup>a</sup>  $\langle E_H \rangle$  is the mean energy of the heavy fission fragment.

<sup>b</sup>  $\langle E_L \rangle$  is the mean energy of the light fission fragment.

<sup>c</sup>  $\langle E_T \rangle$  is the mean measured total kinetic energy.

<sup>d</sup>  $\langle E_K \rangle$  is the mean total kinetic-energy released (neutron corrected).

<sup>e</sup>  $\langle M_L \rangle$  is the mean light-fragment mass distribution.

<sup>f</sup>  $\langle M_H \rangle$  is the mean heavy-fragment mass distribution.

<sup>g</sup>  $\sigma^2( )-d$  are the corresponding variances in the distributions as directly observed together with the value for the Cf<sup>252</sup> calibration, which is given in parenthesis.

<sup>h</sup>  $\sigma^2( )-n$  are the corresponding variances normalized to an arbitrary value for Cf<sup>252</sup>.

<sup>5</sup> J. C. D. Milton and J. S. Fraser, Phys. Rev. **111**, 877 (1958).

<sup>6</sup> H. C. Britt and H. E. Wegner, Los Alamos Scientific Laboratory, University of California, Los Alamos, New Mexico (to be published).

minimized the effect of the  $\sim 10^4$  alpha particles/sec which came from the decay of  $\text{Cm}^{244}$  also present on the foil. The electronic pulses coming from the pre-amplifier were shortened in width from  $\sim 5$  to  $\sim 0.4$   $\mu\text{sec}$ , thus reducing considerably the chance that an accidental alpha particle could add its energy to the measured fission-fragment energy and distort the results. Einsteinium 253 exhibits a very high alpha-to-fission ratio; therefore, the method employing pulse shortening was also used in this experiment (further details are given in Ref. 3).

III. RESULTS

Using the measured energies  $E_1$  and  $E_2$  of both fragments from the fission of a nucleus of mass  $A$ , one can compute the masses  $M_1$  and  $M_2$  and the total kinetic energy  $E_T$  for this event according to

$$M_1/M_2 = E_2/E_1; \quad M_1 + M_2 = A \quad (1)$$

and

$$E_1 + E_2 = E_T. \quad (2)$$

Having recorded 70 000 to 80 000 spontaneous fission events for  $\text{Fm}^{254}$ ,  $\text{Cf}^{254}$ , and  $\text{Cm}^{248}$  and  $\sim 12$  000 events for  $\text{Cf}^{250}$  and  $\text{E}^{253}$ , the results were summarized in the form of two equivalent contour diagrams: (a) the  $E_1$

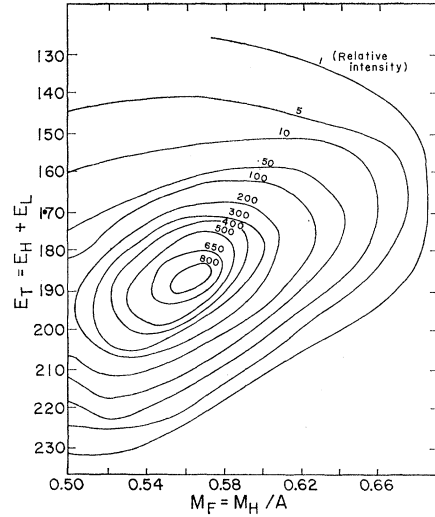
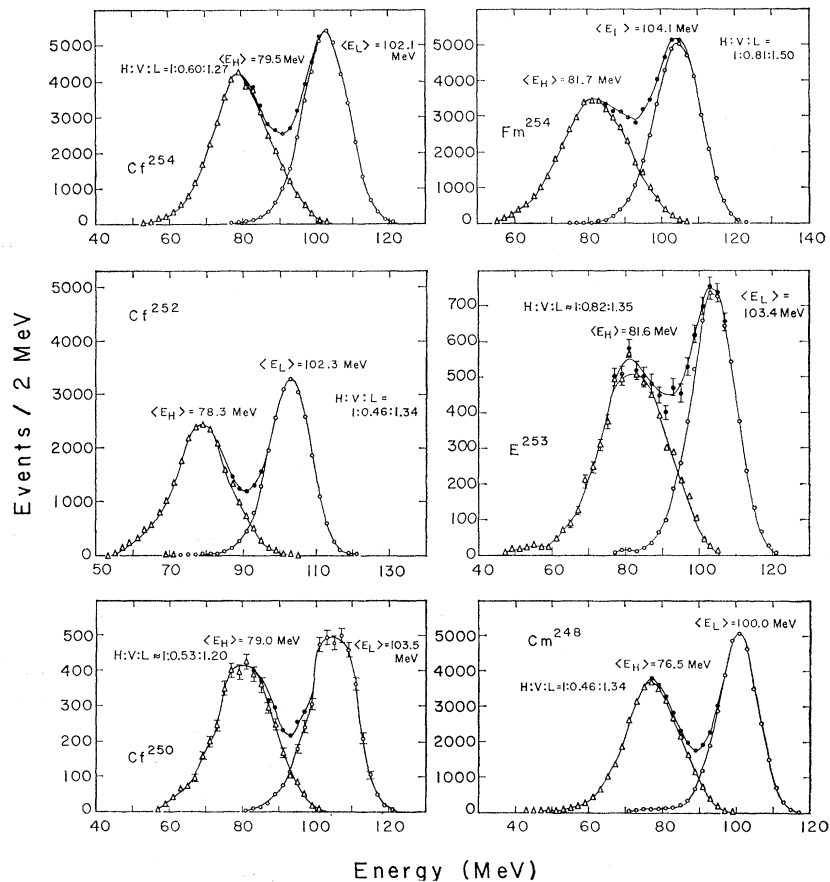


FIG. 1. Contour map in the coordinates  $M_F$  (mass-fraction) and  $E_T$  (total kinetic energy) for  $\text{Fm}^{254}$ . The contours are lines of constant  $N(E_T, M_F)$ .

versus  $E_2$  contour diagram, (b) the  $E_T$  versus  $M_F$  contour diagram, where the "mass-fraction"  $M_F$  equals  $M_1/A$ . Figure 1 shows an example of an  $E_T$  versus  $M_F$  contour diagram for  $\text{Fm}^{254}$ . (None of the contour

FIG. 2. Single fission-fragment energy spectra for the isotopes investigated here. The spectra are subdivided into light- and heavy-fragment spectra.  $H:V:L$  is the ratio of the number of events at the peak of the heavy fragments, at the valley between both peaks, and at the peak of the light fragments.  $\Delta$  heavy fragment,  $\circ$  light fragment,  $\bullet$  both fragments.



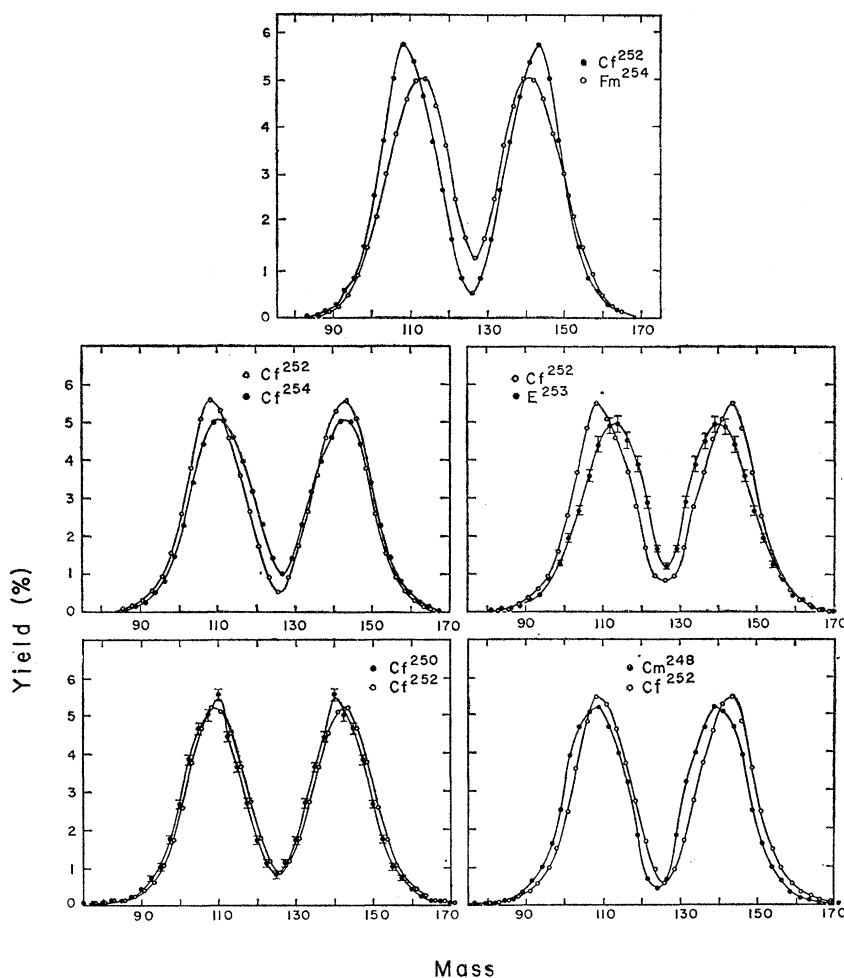


FIG. 3. Mass-yield curve for the isotopes investigated here together with their respective standard  $\text{Cf}^{252}$  mass-yield curves. The statistical errors are either shown or comparable to the size of the points.

diagrams showed any so-called "fine structure," as observed in some other fission studies.<sup>7</sup>) From the two-dimensional contour diagrams we computed (a) single-fragment energy distributions, (b) energy distributions of the heavy fragments  $E_H$ , (c) energy distributions of the light fragments  $E_L$ , (d) distributions of the total kinetic energy  $E_T$ , and (e) mass-yield curves. The mean value and the variance  $\sigma^2$  of each distribution were computed, where  $\sigma^2(E) = \langle E^2 \rangle - \langle E \rangle^2$ . The results of this work are summarized using these two values for each distribution instead of describing the properties of each distribution by its most probable value and its "full width at half-maximum" FWHM (FWHM =  $2.35\sigma$  for a Gaussian distribution). Table II shows the results of these computations. The variances of  $\text{Cf}^{252}$  calibrations differ, because different semiconductor detectors were used which give slightly different results. To compare the variances of all isotopes, we normalized them to one arbitrary value of the variance for  $\text{Cf}^{252}$ .<sup>8</sup> The single-

fission-fragment energy distributions, subdivided also into the light- and heavy-fragment energy distributions are shown in Fig. 2. (The exact corresponding spectra for each  $\text{Cf}^{252}$  calibration are given in Ref. 3.) Figure 3 shows the mass-yield curves with their respective  $\text{Cf}^{252}$  calibrations. An example of the total-kinetic-energy distribution  $E_T$  for  $\text{Fm}^{254}$  is given in Fig. 4.

Figure 5 shows the mean total energy release as a function of the mass fraction  $M_F$  for  $\text{Fm}^{254}$ ,  $\text{E}^{253}$ , and  $\text{Cm}^{248}$ . (In the cases of  $\text{Cf}^{254}$  and  $\text{Cf}^{250}$  these distributions show no significant difference from that of  $\text{Cf}^{252}$ .)

Now let us consider the effects of neutron emission on the experimental results. Most neutrons are emitted after scission.<sup>9,10</sup> Therefore, the emission of neutrons decreases the kinetic energies of the moving fragments and produces an uncertainty in the calculated mass and energy distributions. Only a small number of neutrons are emitted compared to the mass of the

not recorded, only the differences in the variances between the investigated isotopes and  $\text{Cf}^{252}$  are significant.

<sup>9</sup> H. R. Bowman, S. G. Thompson, J. C. D. Milton, and W. J. Swiatecki, Phys. Rev. **126**, 2120 (1962).

<sup>10</sup> H. R. Bowman, J. C. D. Milton, S. G. Thompson, and W. J. Swiatecki, Phys. Rev. **129**, 2133 (1963).

<sup>7</sup> W. M. Gibson, T. D. Thomas, and G. L. Miller, Phys. Rev. Letters **7**, 65 (1961).

<sup>8</sup> Since fission fragments with energies less than  $\sim 50$  MeV were

fragment, and therefore the effect, is small. But the neutron-emission process is very complex, and this introduces a small but very complicated uncertainty into the experimental results. More details concerning these effects are discussed in Appendix A.

Only one correction for the neutron emission can be made easily. The mean prompt kinetic-energy release  $\langle E_K \rangle$  of the "primary fragments" before neutron emission is related to the measured mean total kinetic energy  $\langle E_T \rangle$  of the fission fragments after neutron emission by

$$\langle E_K \rangle = \langle E_T \rangle (1 + \bar{\nu}/A). \quad (3)$$

An estimated value of the average number of neutrons emitted per fission ( $\bar{\nu}$ ), is used for  $\text{Cf}^{250}$ ,  $\text{Cm}^{248}$ , and  $\text{E}^{253}$  on the assumption that  $\bar{\nu}$  increases linearly with  $A$ .<sup>1</sup> The quoted uncertainties in  $\langle E_K \rangle$  include estimates for the variation in energy loss of the fragments due to different thicknesses of the source foils used in the experiments.

#### IV. DISCUSSION

The most essential results of this investigation are summarized as follows:

(a) The energy and mass distributions are rather similar (but not identical) for all isotopes investigated here.

(b) The mean prompt kinetic energy released  $\langle E_K \rangle$  increases with  $Z$  of the fissioning nuclei.

(c) All mass-yield curves show a strong asymmetric mass distribution. In agreement with previously observed trends, the mean heavy-fragment mass is always around  $142 \pm 1$ , whereas the light-fragment mass shows more variation.

(d) Distributions of  $\text{E}^{253}$  which is the first odd-mass isotope investigated resemble very closely those of neighboring even-even nuclei.

(e) The variance of the energy distribution of the heavy fragments  $\sigma^2(E_H)$ , as well as the variance in one branch of the mass-yield curve  $\sigma^2(M)$ , increases with  $Z$  and seems to increase with  $A$  for a given  $Z$ . The variance in the energy distribution of the light fragments  $\sigma^2(E_L)$  is essentially constant.

It would be very interesting to discuss these experimental results in terms of a quantitative theory of fission. However, lacking such a comprehensive theory, we can only compare certain parts of this work with some theoretical considerations concerning a limited aspect of the spontaneous-fission process.

#### A. Mean Prompt Kinetic-Energy Release

It is of interest to compare the mean prompt kinetic energy  $\langle E_K \rangle$  as measured in this work with  $\langle E_K \rangle$  values for other fissioning nuclei. Such a study carried out recently by Viola *et al.* included data for fission induced by heavy ions.<sup>11</sup> (Experimental evidence indicates that

<sup>11</sup> V. E. Viola and T. Sikkeland, Phys. Rev. **130**, 2044 (1963).

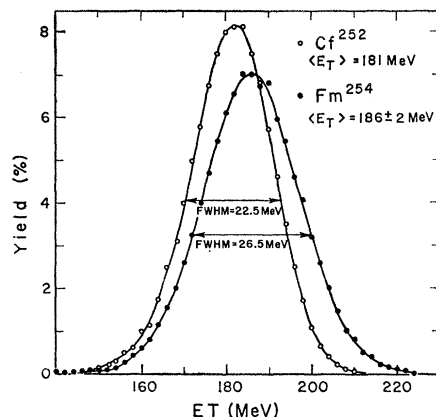


FIG. 4. Total kinetic-energy distribution for  $\text{Fm}^{254}$  together with the standard  $\text{Cf}^{252}$ . (FWHM is full-width at half-maximum.)

$\langle E_K \rangle$  depends only on the nucleus undergoing fission and is independent of its excitation energy.<sup>6,11</sup>)

It may be useful to represent the experimental results in such form that they may be interpreted from a theoretical point of view. Swiatecki<sup>12</sup> suggested that the experimental values might be expressed in terms of  $\xi$  as a function of the fissionability parameter  $X$ :

$$\xi = \langle E_K \rangle / E_s^0 = \langle E_K \rangle / 17.81 A^{2/3} \quad (4)$$

$$X = Z^2 / A / 50.13. \quad (5)$$

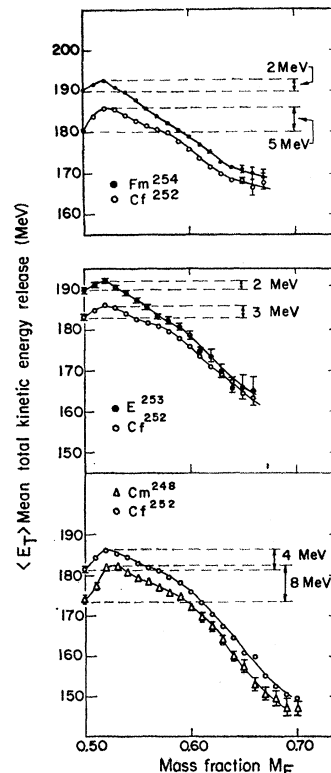


FIG. 5. Mean total kinetic-energy release  $\langle E_T \rangle$  as a function of the mass fraction  $M_F$  for  $\text{Fm}^{254}$ ,  $\text{E}^{253}$ , and  $\text{Cm}^{248}$  as compared to their respective  $\text{Cf}^{252}$  calibrations.

<sup>12</sup> W. J. Swiatecki, Lawrence Radiation Laboratory (private communication).

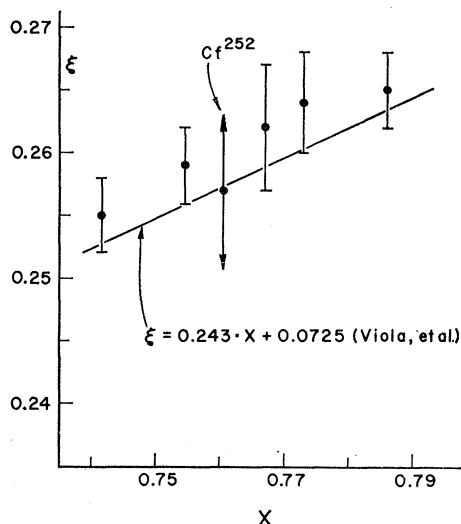


FIG. 6. Mean total kinetic-energy release  $\langle E_K \rangle$  is represented by

$$\xi = \langle E_K \rangle / E_s^0 \quad (E_s^0 = 17.81A^{2/3})$$

and shown as a function of the fissionability parameter  $X$ .  $X = (Z^2/A)/50.13$ . The systematic uncertainty is shown for the standard  $\text{Cf}^{252}$ . For the other cases only errors relative to  $\text{Cf}^{252}$  ( $\langle E_K \rangle = 183 \text{ MeV}$ ) are given.

(Here  $E_s^0$  resembles the nuclear surface energy in terms of the liquid-drop model.)

The straight line representing all other data (Viola *et al.*<sup>11</sup>) is shown in Fig. 6 together with the points representing the experimental results of this work.

The variation in the mean total kinetic energy released  $\langle E_T \rangle$  as a function of the mass fraction  $M_F$  (Fig. 5) is about the same for all the isotopes studied here. However, the decrease in  $\langle E_T \rangle$  for symmetric fission relative to the maximum value of  $\langle E_T \rangle$  tends to decrease for increasing  $Z$ . It should be emphasized that the data in Fig. 5 have not been corrected for experimental dispersions.

### B. Mean Values of the Mass Distribution (Asymmetry)

As mentioned previously, all mass-yield curves show a strong asymmetric distribution. A possible explanation may be in models that have been proposed to explain asymmetry in fission. In attempting to interpret the variation in the degree of asymmetry as a function of  $Z^2/A$ , we consider two models. The first, based on some qualitative features of the liquid-drop model was proposed by Swiatecki.<sup>13</sup> He suggested that the square of the asymmetry should decrease linearly with  $Z^2/A$ , the fissionability parameter. The definition of the asymmetry is arbitrary. Swiatecki used the most probable values of the radiochemical mass-yield curve. Milton suggested that the mean values of the primary

<sup>13</sup> W. J. Swiatecki, *Phys. Rev.* **100**, 936 (1955).

mass distributions would be more adequate to express the over-all picture.<sup>14</sup> Accordingly, the asymmetry can be defined as

$$A_s = (\langle M_H \rangle - \langle M_L \rangle) / A, \quad (6)$$

where  $\langle M_H \rangle$  and  $\langle M_L \rangle$  are the mean values of the heavy- and light-fragment mass distributions, respectively, and  $A$  is the initial mass. The results expressed in this way are shown in Fig. 7(b). Data from the slow-neutron-induced fission of  $\text{U}^{233}$ ,  $\text{U}^{235}$ , and  $\text{Pu}^{239}$  as described by Milton *et al.* are also included.<sup>15</sup> The other data are taken from Hyde's compilation.<sup>1</sup> The relationship between  $A_s^2$  and  $Z^2/A$  is crudely described by a straight line. Recently, Johansson proposed another interpretation of the asymmetry in fission. He used the collective model for which Nilsson calculated the energy levels of the single nucleons at various deformations of the nucleus. Johansson showed that the interaction between levels of opposite parity lower the potential energy when the nucleus is asymmetrically deformed. This implies that the nucleus is asymmetrically deformed at the saddle point and that this asymmetric deformation might be responsible for the asymmetric mass split.<sup>16</sup> On the basis of these considerations Johansson proposed that the mass ratio  $\langle M_H \rangle / \langle M_L \rangle$  should decrease approximately linearly with  $Z^2/A$ .<sup>17</sup> Figure 7(a) shows the experimental data plotted in this way.

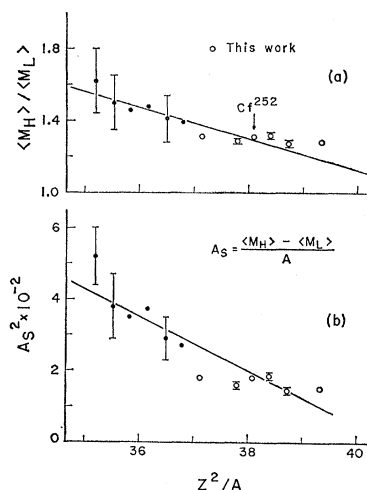


FIG. 7. Change in the asymmetry of the mass-yield curve. (a) Ratio of the mean heavy-fragment mass  $\langle M_H \rangle$  to the mean light-fragment mass  $\langle M_L \rangle$  as a function of  $Z^2/A$ . (b) Square of asymmetry  $A_s^2$  of the mass-yield curve as a function of  $Z^2/A$ . The open circles are points taken from this work. The dots without experimental error represent slow-neutron-induced fission data (Milton and Fraser). The dots with large experimental errors represent cases in which only radiochemical data are available (as compiled by Hyde).

<sup>14</sup> J. C. D. Milton, Chalk River Project, Atomic Energy of Canada Limited, Chalk River, Ontario, Canada (private communication).

<sup>15</sup> J. C. D. Milton and J. S. Fraser, *Can. J. Phys.* **40**, 1626 (1962).

<sup>16</sup> S. A. E. Johansson, *Nucl. Phys.* **22**, 529 (1961).

<sup>17</sup> S. A. E. Johansson, Lawrence Radiation Laboratory (private communication).

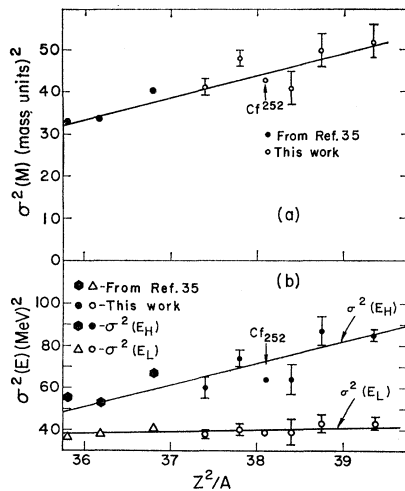


FIG. 8. (a) The variance  $\sigma^2(M)$  in one branch of the mass-yield curve as a function of  $Z^2/A$ . The points are normalized to  $\sigma^2(M)=43$  for  $\text{Cf}^{252}$ . (b) The variance of the heavy-fission-fragment energy spectrum  $\sigma^2(E_H)$  and of the light-fission-fragment energy spectrum  $\sigma^2(E_L)$  as a function of  $Z^2/A$ . The values are uncorrected for neutron emission, but normalized to one (arbitrary) set of values for  $\text{Cf}^{252}$ . Slow-neutron-induced fission data of  $\text{U}^{233}$ ,  $\text{U}^{235}$ , and  $\text{Pu}^{239}$  are included [Milton *et al.* (Ref.15)].

### C. Variances (Widths) of the Distributions

As mentioned above, the variances in the mass and heavy-fragment energy distributions increase with  $Z$  and seem to increase with  $A$ . The variance in the light-fragment energy distribution is essentially constant. We propose to show these variances as functions of  $Z^2/A$  (Fig. 8). We also include the slow-neutron-induced fission data reported by Milton *et al.*<sup>15</sup> An increase in the variance with  $Z^2/A$  can be observed for the mass and heavy-fragment energy distribution. It is also possible to draw a straight line through all these points. This correlation is as good (or bad) as all others in which experimental data such as the spontaneous-fission half-life or asymmetry in the mass distribution is plotted against  $Z^2/A$ .<sup>1</sup>

Since comparably simple features of the fission process, such as the total kinetic-energy release and the asymmetry in the mass distribution, can scarcely be interpreted from a theoretical point of view, we cannot expect to interpret the variances in the distributions. However, one proposal is mentioned which considers qualitatively the trends in the variances of the mass distributions.

Figure 9 shows the asymmetry  $A_S$  as a function of the variance  $\sigma^2(M)$  in one branch of the mass distribution. A large asymmetry is usually accompanied by a small variance and vice versa. As mentioned previously, Johansson suggested that the asymmetry of the mass distribution is connected with an asymmetric deformation of the nucleus at the saddle point. He showed that for large asymmetries the valley in the

potential-energy surface is "sharp," while for small asymmetries the valley is rather "shallow," as represented in Fig. 9. A sharp valley might be connected to a narrow mass distribution, resulting in a small variance, or a shallow valley might be connected with a wide mass distribution and a large variance  $\sigma^2(M)$ , which would account for the general trend in the decrease of  $A_S$  with increasing  $\sigma^2(M)$ .<sup>16,17</sup>

## V. APPENDIXES

### A. Some Effects of Neutron Emission

The solid-state detectors were calibrated for energy with  $\text{Cf}^{252}$ . Time-of-flight measurements of the fission fragments of  $\text{Cf}^{252}$  show that the most probable light fission-fragment energy is  $104.7 \pm 1.0$  MeV for the primary fragments.<sup>5</sup> The light fragment emits an average of 2.1 neutrons.<sup>9</sup> The most probable light-fragment energy measured with solid-state detectors is therefore  $102.9 \pm 1.0$  MeV. On this basis the mean value of the light-fragment energies was found to be  $102.2 \pm 1.0$  MeV. It is easy to compute the mean values of the distribution. Therefore, the detector was calibrated finally in such a way that the mean value for the light-fragment energy distribution of  $\text{Cf}^{252}$  was  $102.2 \pm 0.2$  MeV. Similarly, the most probable heavy-fragment energy was found to be  $78.9 \pm 1.0$  MeV. The mean value used for the calibration was  $78.2 \pm 0.2$  MeV.

The most serious and complicated influence of neutron emission is encountered in attempting to calculate masses from the kinetic energies. Terrell showed recently that neutron emission introduces both a shift in the mass distribution and a dispersion of the mass distribution when fission-fragment masses are

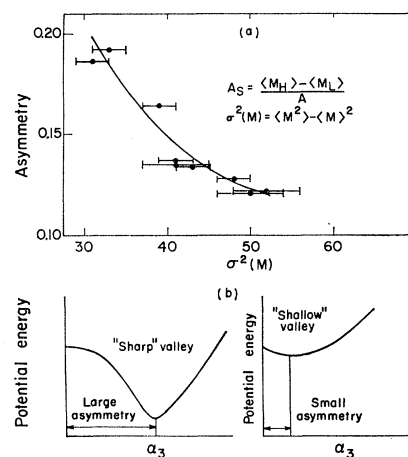


FIG. 9. (a) Asymmetry  $A_S$  as a function of the variance  $\sigma^2(M)$  in one branch of the mass-yield curve. The values are the same as those used for Fig. 8. (b) Qualitative interpretation of Fig. 9(a) as suggested by Johansson (Ref. 17). Potential energy as a function of asymmetric deformation  $\alpha_3$  of the nucleus at the saddle point.

determined by methods employed in this work.<sup>18</sup> However, it has been shown<sup>3</sup> that there exists no quantitative method for deducing the primary mass-yield curve even for Cf<sup>252</sup>. This is due to uncertainties in measurements of the fission-fragment energies and uncertainties in our knowledge of the primary mass-yield curve of Cf<sup>252</sup>.

Therefore, it is premature to attempt to deduce the true primary mass-yield curves for the isotopes investigated in this work. It should be emphasized that the mass-yield curves obtained by radiochemical methods are not directly related to those obtained here; the "radiochemical" mass-yield curves are shifted but not dispersed due to neutron emission. The mass-yield results reported here are distorted primary mass-yield distributions.

### B. Approximate Treatment of the Total Energy Balance

If one assumes that all neutrons are emitted from the separated fragments, the total energy release  $T_E$  in a fission event is

$$T_E = E_K + E_X, \quad (\text{A1})$$

where  $E_X$  is the internal excitation energy of both fragments and  $E_K$  is the kinetic energy of the fully accelerated primary fission fragments. The excitation energy of the fragments is lowered by the emission of a number of neutrons  $\nu$ , each neutron reducing the excitation energy by the kinetic energy  $E_N$  it carries off and by its neutron binding energy  $E_B$ . The excitation energy is also lowered by the emission of gamma rays; this energy is  $E_G$ . Therefore, we have for one fission event

$$E_X = E_G + \sum_{n=1}^{\nu} [E_N(n) + E_B(n)]. \quad (\text{A2})$$

Averaged in weighted form over all possible fission modes, the total energy balance can be written as

$$\langle T_E \rangle = \langle E_K \rangle + \bar{\nu} \langle E_B \rangle + \langle E_N \rangle + \langle E_G \rangle. \quad (\text{A3})$$

The average total energy release  $\langle T_E \rangle$  for the isotopes considered here was calculated using Milton's recently

TABLE III. Energy balance in spontaneous fission.

Isotope	$\langle T_E \rangle^a$ (MeV)	$\langle E_X \rangle^b$ (MeV)	$\langle E_B \rangle^c$ (MeV)	$\bar{\nu}_{\text{exptl}}^d$	$D = \langle T_E \rangle - \langle T_C \rangle$ (MeV)
Fm <sup>254</sup>	230.4	41.7	5.63	4.05	+5
E <sup>253</sup>	225.0	37.1	5.46	3.9 <sup>e</sup>	+2
Cf <sup>254</sup>	216.5	32.0	5.01	3.9	-2
Cf <sup>252</sup>	216.1	33.2	5.16	3.8	-1
Cf <sup>250</sup>	216.8	32.0	5.43	3.5 <sup>e</sup>	-1
Cm <sup>248</sup>	204.9	26.0	5.05	3.3 <sup>e</sup>	-4

<sup>a</sup>  $\langle T_E \rangle$  is the mean total energy release.

<sup>b</sup>  $\langle E_X \rangle$  is the mean fragment excitation energies.

<sup>c</sup>  $\langle E_B \rangle$  is the mean neutron binding energy.

<sup>d</sup>  $\bar{\nu}$  is the mean number of neutrons emitted.

<sup>e</sup> Estimated value.

computed energy-release values for each pair of fragment masses.<sup>19</sup> The mass-yield curves were taken from the present work. Also we have computed the  $T_E$  values from the right-hand side of Eq. (A3) and denote the result with  $\langle T_C \rangle$ . Here  $\langle E_K \rangle$  is measured experimentally,  $\bar{\nu}$  is either known experimentally or estimated as previously mentioned,  $\langle E_B \rangle$  can again be computed by using Milton's tables,<sup>19</sup>  $\langle E_N \rangle$  is known experimentally for Cf<sup>252</sup> and assumed to be equal for all isotopes investigated,<sup>9,10</sup> and  $\langle E_G \rangle$  is assumed to be 8.5 MeV for all investigated isotopes.

Table III shows the results of these calculations. The last column contains the difference  $D$  between  $\langle T_E \rangle$  and  $\langle T_C \rangle$ . It is interesting that the agreement between  $\langle T_E \rangle$  and  $\langle T_C \rangle$  is better than could be expected in view of the uncertainties in the measurements and the assumptions that were made.

### ACKNOWLEDGMENTS

We are grateful to Dr. W. J. Swiatecki for help in the conception of this work and for many helpful discussions. We also wish to thank Dr. S. A. E. Johansson for his help in interpreting the experimental results.

We are grateful to Professor Isadore Perlman for his continuous interest in the work reported here.

We also wish to thank L. Gibson for his help with the electronic equipment, W. Hansen for supplying the solid-state detectors, and Mrs. J. Rees for her help in preparing this manuscript.

<sup>19</sup> J. C. D. Milton, Lawrence Radiation Laboratory Report UCRL-9883 revised, 1962 (unpublished).

<sup>18</sup> J. Terrell, Phys. Rev. **127**, 880 (1962).